Intermittency transition to generalized synchronization in coupled time-delay systems

D. V. Senthilkumar[1]* and M. Lakshmanan[1]†
[1] *Centre for Nonlinear Dynamics, Department of Physics, Bharathidasan University, Tiruchirapalli - 620 024, India*

(Dated: February 2, 2008)

In this paper, we report the nature of transition to generalized synchronization (GS) in a system of two coupled scalar piecewise linear time-delay systems using the auxiliary system approach. We demonstrate that the transition to GS occurs via on-off intermittency route and also it exhibits characteristically distinct behaviors for different coupling configurations. In particular, the intermittency transition occurs in a rather broad range of coupling strength for error feedback coupling configuration and in a narrow range of coupling strength for direct feedback coupling configuration. It is also shown that the intermittent dynamics displays periodic bursts of period equal to the delay time of the response system in the former case, while they occur in random time intervals of finite duration in the latter case. The robustness of these transitions with system parameters and delay times has also been studied for both linear and nonlinear coupling configurations. The results are corroborated analytically by suitable stability conditions for asymptotically stable synchronized states and numerically by the probability of synchronization and by the transition of *sub*Lyapunov exponents of the coupled time-delay systems. We have also indicated the reason behind these distinct transitions by referring to unstable periodic orbit theory of intermittency synchronization in low-dimensional systems.

PACS numbers: 05.45.Xt,05.45.Pq

I. INTRODUCTION

Synchronization of interacting chaotic oscillators is one of the most interesting nonlinear phenomenon and is an inherent part of many natural systems (cf.[1, 2]). The concept of synchronization is receiving a central importance in recent research in nonlinear dynamics due to its potential applications in diverse areas of science and technology. Since the identification of chaotic synchronization [3, 4, 5], several works have appeared in identifying and demonstrating basic kinds of synchronization both theoretically and experimentally [1, 2, 3, 4, 5]. There are also attempts to find a unifying framework for defining the overall class of chaotic synchronizations [6, 7, 8].

One of the interesting synchronization behaviors of unidirectionally coupled chaotic systems is the generalized synchronization (GS), which was conceptually introduced in Ref. [9]. Generalized synchronization is observed in coupled nonidentical systems, where there exists some functional relation between the drive $X(t)$ and the response $Y(t)$ systems, that is, $Y(t) = F(X(t))$. With GS, all the response systems coupled to the drive lose their intrinsic chaoticity (sensitivity to initial conditions) under the same driving and follow the same trajectory. Hence the presence of GS can be detected using the so called auxiliary system approach [10], where an additional system (auxiliary system) identical to the response system is coupled to the drive in similar fashion. Auxiliary system approach is particularly appealing since it can be implemented directly in an experiment and, in addition, this method allows one to utilize analytical approaches for studying GS. However, one has to be aware that if there are multiple basins of attraction for the coupled drive-response system, then the auxiliary system approach can fail.

Generalized synchronization (GS) has been well studied and understood in systems with few degrees of freedom and for discrete maps [9, 10, 11, 12, 13, 14, 15]. The concept of GS has also been extended to spatially extended chaotic systems such as coupled Ginzburg-Landau equations [16]. Recently, the terminology intermittent generalized synchronization (IGS) [17] was introduced in diffusively coupled Rössler systems in analogy with intermittent lag synchronization (ILS) [18, 19] and intermittent phase synchronization (IPS) [20, 21, 22], and also experimentally in coupled Chua's circuit. Very recently, it has been shown [23] that the transition to intermittent chaotic synchronization (in the case of complete synchronization) is characteristically distinct for geometrically different chaotic attractors. In particular, it has been shown that for phase coherent chaotic attractors (Rössler attractor) the transition occurs immediately as soon as the coupling strength is increased from zero and for non-phase-coherent attractors (Lorenz attractor), the transition occurs slowly as the coupling is increased from zero.

Time-delay systems form an important class of dynamical systems and recently they are receiving central importance in investigating the phenomenon of chaotic synchronizations in view of their infinite dimensional nature and feasibility of experimental realization [24, 25, 26, 27].

*Electronic address: skumar@cnld.bdu.ac.in
†Electronic address: lakshman@cnld.bdu.ac.in

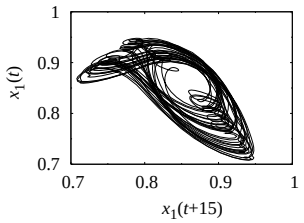

FIG. 1: The hyperchaotic attractor of the system (1) for the parameter values $a = 1.0, b = 1.2$ and $\tau = 15.0$.

While the concept of GS has been well established in low dimensional systems, it has not yet been studied in detail in coupled time-delay systems and only very few recent studies have been dealt with GS in time-delay systems [24, 25]. In particular, the mechanism of onset of GS in coupled time-delay systems and its characteristic properties have not yet been clearly understood and require urgent attention.

In this paper, we investigate the characteristic properties of nature of onset of GS from asynchronous state in unidirectionally coupled piece-wise linear time-delay systems exhibiting highly non-phase coherent hyperchaotic attractors [26]. We find that the onset of GS is preceded by on-off intermittency mechanism from the desynchronized state. We have also identified that the intermittency transition to GS exhibits characteristically distinct behaviors for different coupling schemes. In particular, the intermittency transition occurs in a broad range of coupling strength for error feedback coupling configurations and in a narrow range of coupling strength for direct feedback coupling configurations, beyond certain threshold value of coupling strength. In addition, the intermittent dynamics is characterized by periodic bursts away from the temporal synchronized state with period equal to the delay time of the response system in the case of broad range intermittency transition whereas it is characterized by random time intervals in the case of narrow range intermittency transition. We have also confirmed these dynamical behaviours in both linear and nonlinear coupling configurations. We have analyzed these transitions analytically using Krasvoskii-Lyapunov functional approach and numerically by the probability of synchronization and by the *sub*Lyapunov exponents. We have also addressed the reason behind these transitions using periodic orbit theory. The robustness of these transitions with the system parameters in both the linear and nonlinear, error feedback and direct feedback coupling configurations, are also studied.

The plan of the paper is as follows. In Sec. II, we will point out the existence of broad range intermittency transition to GS for linear error feedback coupling proportional to $(x_1(t) - x_2(t))$ while in Sec. III the existence of narrow range intermittency transition is shown for the linear direct feedback coupling of the form $x_1(t)$, where $x_1(t)$ and $x_2(t)$ are the drive and response signals, respectively (see below for details). In Sec. IV we will discuss the existence of broad range intermittency transition for nonlinear error feedback coupling of the form $(f(x_1(t-\tau_2)) - f(x_2(t-\tau_2)))$, where $f(x)$ is an odd piece-wise linear function. The existence of narrow range intermittency transition is discussed in Sec. V for nonlinear direct feedback coupling of the form $(f(x_1(t-\tau_2))$. Finally in Sec. VI, we will summarize our results.

II. BROAD RANGE (SLOW/DELAYED) INTERMITTENCY TRANSITION TO GS FOR LINEAR ERROR FEEDBACK COUPLING OF THE FORM $(x_1(t) - x_2(t))$

We consider the following first order delay differential equation introduced by Lu and He [28] and discussed in detail by Thangavel et al. [29],

$$\dot{x}(t) \;=\; -ax(t) + bf(x(t-\tau)), \tag{1}$$

where a and b are parameters, τ is the time-delay and f is an odd piecewise linear function defined as

$$f(x) = \begin{cases} 0, & x \le -4/3 \\ -1.5x - 2, & -4/3 < x \le -0.8 \\ x, & -0.8 < x \le 0.8 \\ -1.5x + 2, & 0.8 < x \le 4/3 \\ 0, & x > 4/3. \end{cases} \tag{2}$$

Recently, we have reported [30] that the system (1) exhibits hyperchaotic behavior for suitable parametric values. For our present study, we find that for the choice of the parameters $a = 1.0, b = 1.2$ and $\tau = 15.0$ with the initial condition $x(t) = 0.9, t \in (-5, 0)$, Eq. (1) exhibits hyperchaos. The corresponding pseudoattractor is shown in Fig. 1. The hyperchaotic nature of Eq. (1) is confirmed by the existence of multiple positive Lyapunov exponents. The first ten maximal Lyapunov exponents for the above choice of parameters as a function of delay time τ is shown in Fig. 2 (spectrum of Lyapunov exponents in this paper are calculated using the procedure suggested by Farmer [31]).

To be specific, we first consider the following unidirectional, linearly coupled systems with drive $x_1(t)$, response $x_2(t)$ and an auxiliary $x_3(t)$,

$$\dot{x}_1(t) = -ax_1(t) + b_1 f(x_1(t-\tau_1)), \tag{3a}$$

$$\dot{x}_2(t) = -ax_2(t) + b_2 f(x_2(t-\tau_2)) + b_3(x_1(t) - x_2(t)), \tag{3b}$$

$$\dot{x}_3(t) = -ax_3(t) + b_2 f(x_3(t-\tau_2)) + b_3(x_1(t) - x_3(t)), \tag{3c}$$

where b_1, b_2 and b_3 are constant parameters, and τ_1 and τ_2 are constant delay parameters. Note that when $b_1 \neq b_2$ or $\tau_1 \neq \tau_2$ or both, corresponding to parameter mismatches, we have unidirectionally coupled nonidentical systems (Eq. (3a) and (3b)), while the auxiliary system is given by (3c) and $f(x)$ is the odd piece-wise linear

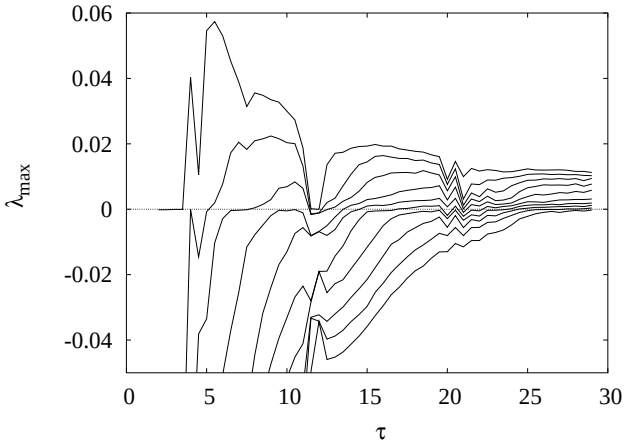

FIG. 2: The first ten maximal Lyapunov exponents λ_{max} of the scalar time-delay system for the parameter values $a = 1.0, b_1 = 1.2, \tau \in (2, 29)$ (which is the same as Eq. (1) with b_1 replaced by b) (3a).

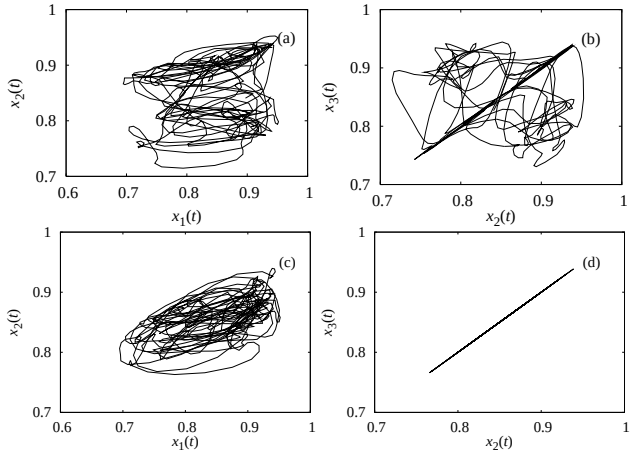

FIG. 3: Dynamics in the phase space of the systems (3). (a) and (b): Approximate GS and CS, respectively, for the value of the coupling strength $b_3 = 0.4$. (c) and (d): Perfect GS and CS, respectively, for the value of the coupling strength $b_3 = 0.9$.

function (2). The coupling in (3b) may be also called a linear error feedback coupling.

For simplicity, we have chosen $b_1 = b_2$ so that the time-delays τ_1 and τ_2 alone introduce a simple form of parameter mismatch between the drive $x_1(t)$ and the response $x_2(t)$. We have chosen the values of parameters as $a = 1.0, b_1 = b_2 = 1.2, \tau_1 = 20$ and $\tau_2 = 25$. For this parametric choice, in the absence of coupling, all the three systems (3) evolve independently and exhibit hyperchaotic attractors, which is confirmed by the existence of multiple positive Lyapunov exponents (Fig. 2). The actual value of the positive Lyapunov exponents for $\tau = 20$ are 0.00916, 0.00759, 0.00565, 0.00283 and 0.00073 and for $\tau = 25$ they are 0.01234, 0.01067, 0.00886, 0.00658, 0.00386, 0.00229, 0.00123 and 0.00033.

A. Stability Condition

With GS, as all the response systems under the same driving follow the same trajectory, it is sufficient to identify the existence condition for establishment of complete synchronization (CS) between the response $x_2(t)$ and the auxiliary $x_3(t)$ systems in order to achieve GS between the drive $x_1(t)$ and the response $x_2(t)$ systems.

Now, for CS to occur between the response $x_2(t)$ and the auxiliary $x_3(t)$ variables, we consider the time evolution of the difference system with the state variable $\Delta = x_3(t) - x_2(t)$. It can be written for small values of Δ as

$$\dot{\Delta} = -(a + b_3)\Delta + b_2 f'(x_2(t - \tau_2))\Delta_{\tau_2}, \tag{4}$$

where

$$f'(x) = \begin{cases} -1.5, & -4/3 < x \leq -0.8 \\ 1, & -0.8 < x \leq 0.8 \\ -1.5, & 0.8 < x \leq 4/3. \end{cases} \tag{5}$$

The synchronization manifold, $x_2(t) = x_3(t)$, is locally attracting if the origin of this equation is stable. Following Krasovskii-Lyapunov functional approach, we define a positive definite Lyapunov functional of the form [27, 32, 33] (details of stability analysis are given in appendix A)

$$V(t) = \frac{1}{2}\Delta^2 + \mu \int_{\tau_2}^{0} \Delta^2(t + \theta)d\theta, \tag{6}$$

where μ is an arbitrary positive parameter, $\mu > 0$. The solution of Eq. (4), namely $\Delta = 0$, is stable if the derivative of the functional along the trajectory of Eq. (4) is negative. This negativity condition is satisfied if $b_3 + a > \frac{b_2^2 f'^2(x_2(t-\tau_2))}{4\mu} + \mu$, from which it turns out that the sufficient condition for asymptotic stability is

$$a + b_3 > |b_2 f'(x_2(t - \tau_2))|\,. \tag{7}$$

Now from the form of the piecewise linear function $f(x)$ given by Eq. (2), we have,

$$|f'(x_2(t - \tau_2))| = \begin{cases} 1.5, & 0.8 \leq |x_2| \leq \frac{4}{3} \\ 1.0, & |x_2| < 0.8. \end{cases} \tag{8}$$

Consequently the stability condition (7) becomes $a+b_3 > |1.5b_2| > |b_2|$. Thus one can take

$$a + b_3 > |b_2| \tag{9}$$

as the less stringent or approximate stability condition (as the synchronization dynamics of the coupled systems (3) can occur even beyond the inner region, $|x_2| < 0.8$) for (7) to be valid, while

$$a + b_3 > |1.5b_2| \tag{10}$$

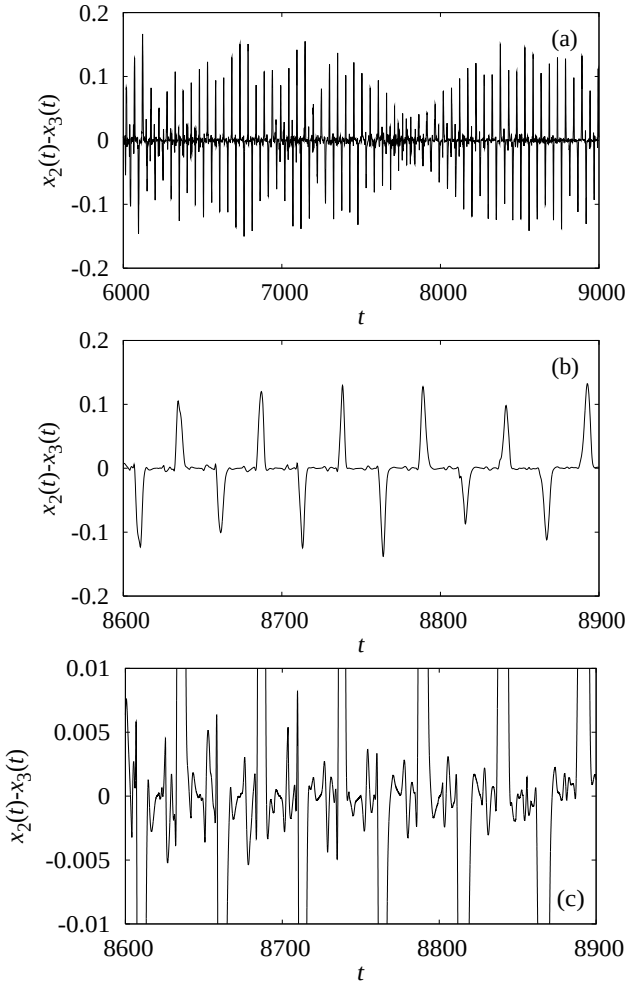

FIG. 4: The intermittent dynamics of the response $x_2(t)$ and auxiliary $x_3(t)$ systems for the value of the coupling strength $b_3 = 0.4$. (a) Time traces of the difference $x_2(t) - x_3(t)$ corresponding to Fig. 3b, (b) Enlarged in x scale to show bursts at periodic intervals when bursts of larger amplitudes $\Delta > |0.01|$ are considered and (c) Enlarged in y scale to show random bursts when bursts of smaller amplitudes $\Delta < |0.01|$ are considered.

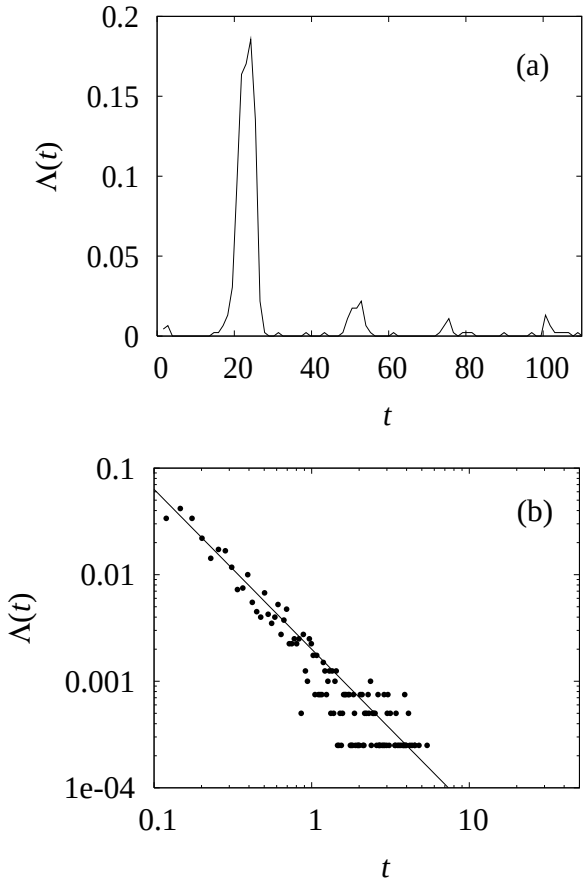

FIG. 5: The statistical distribution of laminar phases corresponding to the Fig. 4. (a) For threshold value $\Delta = |0.1|$ and (b) for the threshold value of $\Delta = |0.0001|$.

can be considered as the most general or stringent or exact stability condition (as the full synchronization dynamics of the coupled systems (3) lies within the outer region $0.8 < |x_2| \leq \frac{4}{3}$) specified by (7) for asymptotic stability of the synchronized state $\Delta = 0$.

B. Approximate (Intermittent) Generalized Synchronization

In order to understand the mechanism of transition to synchronized state, it will be important to follow the dynamics from the parameter values at which the less stringent condition is satisfied. Figure 3a shows the approximate GS (which may also be termed as intermittent generalized synchronization (IGS) in analogy with intermittent lag synchronization (ILS)) between the drive $x_1(t)$ and the response $x_2(t)$ systems, whereas Fig. 3b shows the approximate CS between the response $x_2(t)$ and the auxiliary $x_3(t)$ systems for the values of the parameters $a = 1.0, b_1 = b_2 = 1.2, \tau_1 = 20, \tau_2 = 25$ and $b_3 = 0.4$ satisfying the less stringent condition (9). Perfect GS and perfect CS are shown in Figs. 3c and 3d respectively for $b_3 = 0.9$ satisfying the general stability condition (10). Time traces of the difference $x_2(t) - x_3(t)$ corresponding to approximate CS (Fig. 3b) are shown in Fig. 4, which show periodic bursts with period between two consecutive bursts approximately equal to the time-delay of the response system $t \approx 25$ when 'on' states of amplitude greater than $|0.01|$ are considered. Fig. 4b shows an enlarged (in x scale) part of Fig. 4a to view the bursts at periodic intervals when bursts of larger amplitudes ($\Delta > |0.01|$) are considered, while Fig. 4c is an enlarged (in y scale) version of Fig. 4b to show random bursts when bursts of smaller amplitude $\Delta < |0.01|$ are considered.

Usually the intermittent dynamics is characterized by the entrainment of the dynamical variables in random

time intervals of finite duration [34, 35]. But from Fig. 4b, it is evident that the intermittent dynamics displays periodic bursts from the synchronous state with period approximately equal to the delay time of the response system, when amplitudes of the state variable $|\Delta| = |x_3(t) - x_2(t)| > 0.01$ are considered, for the values of the coupling strength at which the less stringent stability condition (9) is satisfied. The statistical features associated with the intermittent dynamics is analyzed by calculating the distribution of laminar phases $\Lambda(t)$ with amplitude less than a threshold value to Δ. A universal asymptotic power law distribution $\Lambda(t) \propto t^{-\alpha}$ is observed for the threshold value $\Delta = |0.0001|$ with the value of the exponent $\alpha = -1.5$ as shown in Fig. 5b, which is quite typical for on-off intermittency. On the other hand the distribution of laminar phases $\Lambda(t)$ for the value of the threshold value of $|\Delta = 0.1|$ shows a periodic structures (Fig. 5a), where the peaks occur approximately at $t = nT, n = 1, 2, ...$, where $T \approx \tau_2$ is the period of the lowest periodic orbit of the uncoupled system (3b). Note that $-3/2$ power law is observed for the intermittent dynamics shown in Fig. 4 for laminar phases $\Lambda(t)$ with amplitude less than $\Delta = |0.0001|$ (as an illustrative example), which is also evident from Fig. 4c, while periodic bursts are observed for 'on' state of amplitude greater than $|0.01|$. It is to be noted that such periodic bursts of period approximately equal to the time-delay of the response system for larger threshold value of Δ along with the on-off intermittency behavior for larger threshold value of Δ has also been observed by Zhan *et al* [24] in unidirectionally coupled Mackey-Glass systems , where the authors discussed relation between two modes of synchronization, namely, CS and GS.

C. Characterization of IGS

Now we characterize the intermittency transition to GS by using (i) the notion of the probability of synchronization $\Phi(b_3)$ as a function of the coupling strength b_3 [23], which can be defined as the fraction of time during which $|x_2(t) - x_3(t)| < \epsilon$ occurs, where ϵ is a small but arbitrary threshold, and (ii) from the changes in the sign of *sub*Lyapunov exponents (which are nothing but the Lyapunov exponents of the subsystem) in the spectrum of Lyapunov exponents of the coupled time-delay systems. Fig. 6a shows the probability of synchronization $\Phi(b_3)$ as a function of the coupling strength b_3 calculated from the variables of the response $x_2(t)$ and the auxiliary $x_3(t)$ systems for CS between them. For the range of $b_3 \in (0, 0.39)$, there is absence of any entrainment between the systems resulting in asynchronous behavior and the probability of synchronization $\Phi(b_3)$ is practically zero in this region. However, starting from the value of $b_3 = 0.39$ and above, there appear oscillations in the value of the probability of synchronization $\Phi(b_3)$ between zero and some finite values less than unity, exhibiting intermittency transition to GS in the range of

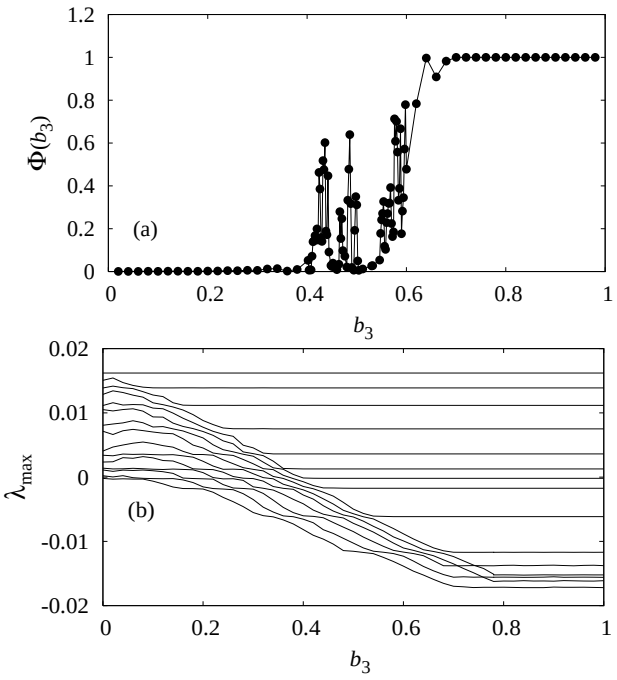

FIG. 6: (a) The probability of synchronization $\Phi(b_3)$ between the response $x_2(t)$ and the auxiliary $x_3(t)$ systems and (b) Largest Lyapunov exponents of the coupled drive $x_1(t)$ and response $x_2(t)$ systems (3a) and (3b).

$b_3 \in (0.4, 0.62)$ for which the less stringent stability condition (9) is satisfied. Beyond $b_3 = 0.62$, $\Phi(b_3)$ attains unit value indicating perfect GS. Note that the above intermittency transition occurs in a rather wide range of the coupling strength (this can also be termed as slow or delayed intermittency transition in analogy with the terminology used in [23]), which has also been confirmed from the transition of successive largest *sub*Lyapunov exponents in the corresponding range of the coupling strength.

The spectrum of the first fifteen largest Lyapunov exponents λ_{max} of the coupled drive $x_1(t)$ and response $x_2(t)$ systems are shown in Fig. 6b. From the general stability condition (7), it is evident that for the chosen value of the parameter $a = 1.0$, the less stringent stability condition (9) is satisfied for the values of coupling strength $b_3 > 0.2$. Correspondingly, the least positive *sub*Lyapunov exponent of the response system (3b) gradually becomes negative from $b_3 > 0.2$. Subsequently, the remaining positive *sub*Lyapunov exponents gradually become negative and attain saturation in the range of $b_3 \in (0.2, 0.8)$. This is in accordance with the fact that the less stringent stability condition is satisfied only in the corresponding range of coupling strength b_3. This is a strong indication of the broad range intermittency (IGS) transition to GS. For $b_3 > 0.8$, the general stability condition (10) is satisfied, where one can observe perfect GS as is evidenced by both the probability of synchronization approaching unit value and by the negative

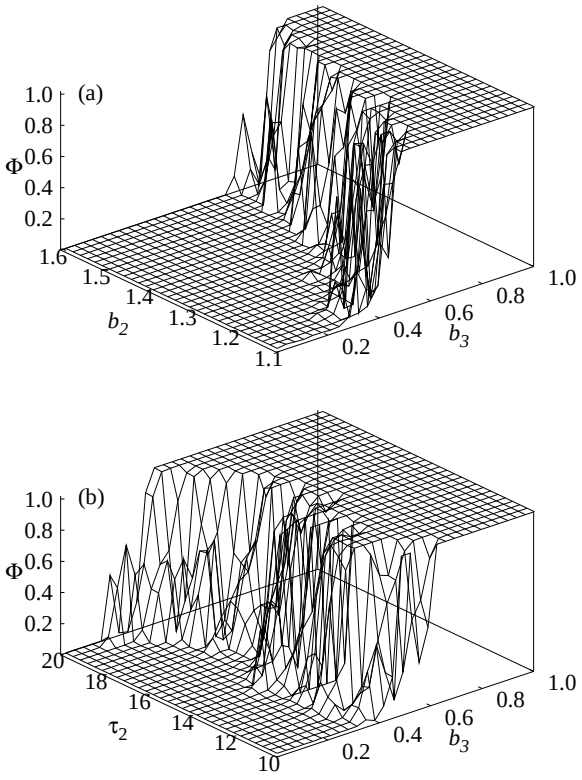

FIG. 7: The probability of synchronization $\Phi(b_3)$ in 3-dimensional plots (a) as a function of the system parameter b_2 and the coupling strength b_3 and (b) as a function of the coupling delay τ_2 and the coupling strength b_3, exhibiting broad range intermittency transition to GS for linear error feedback coupling.

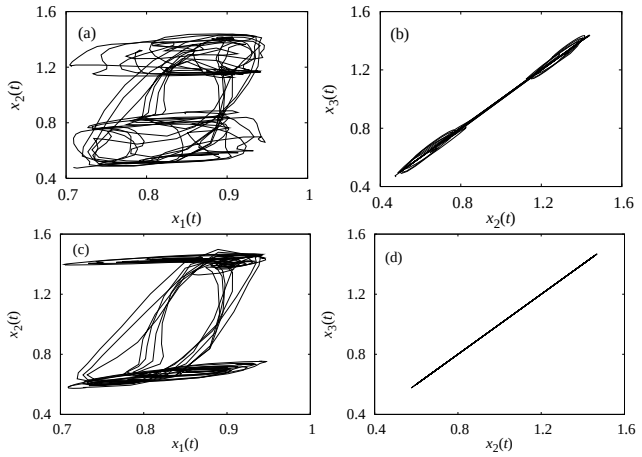

FIG. 8: Dynamics in the phase space of the systems (11): (a) and (b) Approximate GS and CS, respectively, for the value of the coupling strength $b_3 = 0.64$ and (c), (d) Perfect GS and CS, respectively, for the value of the coupling strength $b_3 = 0.8$.

saturation of *sub*Lyapunov exponents calculated between the drive and response systems. The inference is that the correlation between the oscillations of the systems eventually becomes stronger with the strength of the coupling, and this is indicated by the successive transition of *sub*Lyapunov exponents to negative values.

It is a well established fact that a chaotic attractor can be considered as a pool of infinitely many unstable periodic orbits of all periods. Synchronization between two coupled systems is said to be asymptotically stable, if all the unstable periodic orbits of the response system are stabilized in the transverse direction of the synchroniation manifold. Consequently, all the trajectories transverse to the synchronization manifold converge for suitable values of coupling strength and this is reflected in the negative values of the transverse Lyapunov exponents (*sub*Lyapunov exponents) upon synchronization [23]. From our results, we find that the *sub*Lyapunov exponents gradually become negative in a broad range of coupling strength b_3 after certain threshold value and this is in accordance with the known results on gradual stabilization of unstable periodic orbits of the response system in the complex synchronization manifold of low dimensional systems [23]. Unfortunately, methods for locating UPO's and calculating their transverse Lyapunov exponents have not been well established for time-delay systems and hence a quantitative proof for the gradual stabilization of UPO's has not been given here. However, the gradual stabilization of UPO's along with their transverse Lyapunov exponent in the range of intermittency transition have been reported for the case of coupled Rössler and Lorenz systems in Ref. [23]. It can then be inferred from these studies that the broad range intermitteny transition in the case of error feedback coupling configuration is due to the fact that the strength of the coupling b_3 contributes only less significantly to stabilize the UPO's as the error $x_1(t) - x_2(t)$ gradually becomes smaller from the transition regime after certain threshold value of the coupling strength.

The robustness of the intermittency transition in a broad range of coupling strength with the system parameter $b_2 \in (1.1, 1.6)$ and with the coupling delay $\tau_2 \in (10, 20)$ has also been confirmed. Fig. 7a shows the 3-dimensional plot of the probability of synchronization as a function of the system parameter b_2 and the coupling strength b_3, while Fig. 7b shows the 3-dimensional plot of $\Phi(b_3)$ as a function of the coupling delay τ_2 and the coupling strength b_3. The above figures (Fig. 7) clearly reveal the broad range intermittency transition to GS in the case of linear error feedback coupling scheme.

III. NARROW RANGE (IMMEDIATE) INTERMITTENCY TRANSITION TO GS FOR LINEAR DIRECT FEEDBACK COUPLING OF THE FORM $x_1(t)$

To illustrate the narrow range intermittency transition to GS, we consider the unidirectional linear direct feedback coupling of the form

$$\dot{x}_1(t) = -ax_1(t) + b_1 f(x_1(t-\tau_1)), \quad (11a)$$
$$\dot{x}_2(t) = -ax_2(t) + b_2 f(x_2(t-\tau_2)) + b_3 x_1(t), \quad (11b)$$
$$\dot{x}_3(t) = -ax_3(t) + b_2 f(x_3(t-\tau_2)) + b_3 x_1(t), \quad (11c)$$

where $f(x)$ is of the same odd piece-wise linear form as in Eq. (2). Assuming the same values of the parameters as before and proceeding in the same way as in the previous case, one can obtain the sufficient condition for asymptotically stable CS between the response $x_2(t)$ (11b) and the auxiliary $x_3(t)$ (11c) systems as

$$a > |b_2 f'(x_2(t-\tau_2))|\,. \quad (12)$$

It is to be noted that the above stability condition holds good only for the case when coupling is present, that is $b_3 \neq 0$. When there is no coupling ($b_3 = 0$), by definition, there will be a desynchronized chaotic state. As soon as the value of the coupling strength is increased from zero, the stability condition (12) always lead to synchronized state even for very feeble values of b_3 for parameters satisfying the stability condition, as it is independent of the coupling strength b_3. As the values of the parameters satisfying the stability condition (12) rapidly leads to immediate transition to synchronized state as soon as the coupling is switched on, it is difficult to identify the possible transitions to synchronized state. In addition, as the stability condition is independent of the coupling strength b_3, one is not able to explore the dynamical transitions as a function of coupling strength for the parameter values satisfying the stability condition (12). Hence we study the synchronization transition by choosing the parameters violating the stability condition as $a = 1.0, b_1 = 1.2, b_2 = 1.1, \tau_1 = \tau_2 = 20$ and varying the coupling strength b_3 in order to identify the mechanism of synchronization transition. Here, in this case b_1 and b_2 alone introduce the parameter mismatch while $\tau_1 = \tau_2$ (It may be added that the qualitative nature of the dynamical transitions remain the same even when the mismatch is either in time delays alone, that is $\tau_1 \neq \tau_2$, $b_1 = b_2$ or in both the system parameters and time delays, $b_1 \neq b_2$, $\tau_1 \neq \tau_2$, as confirmed below in the three dimensional plots of Figs. 12).

As b_3 is varied from zero, transition from desynchronized state to approximate GS occurs for $b_3 > 0.6$. Approximate GS (IGS) between the drive system $x_1(t)$ specified by Eq. (11a), and the response system $x_2(t)$ represented by Eq. (11b), is shown in Fig. 8a whereas the approximate CS between the response $x_2(t)$ (Eq. (11b)) and the auxiliary $x_3(t)$ (Eq. (11c)) systems is shown in Fig. 8b for the value of the coupling strength $b_3 = 0.64$.

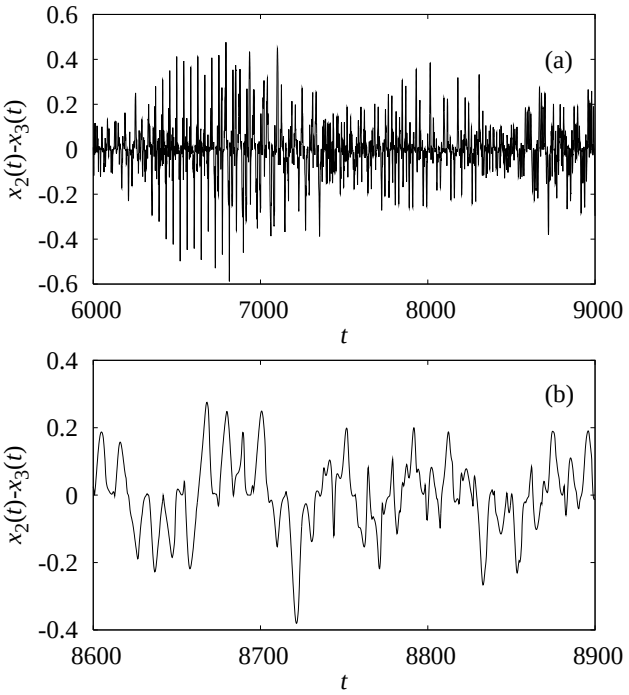

FIG. 9: The intermittent dynamics of the response $x_2(t)$ (11b) and auxiliary $x_3(t)$ (11c) systems for the value of the coupling strength $b_3 = 0.64$. (a) and (b) Time traces of the difference $x_2(t) - x_3(t)$ corresponding to Fig. 8b.

Prefect GS and CS are shown in Figs. 8c and 8d, respectively, for the value of the coupling strength $b_3 = 0.8$. The intermittent dynamics at the transition regime corresponding to the value of the coupling strength $b_3 = 0.64$ is shown in Figs. 9, in which Fig. 9b shows the enlarged part of Fig. 9a. It is clear from this figure that the intermittent dynamics displays intermittent bursts at random time intervals. The statistical distribution of the laminar phases again shows a universal asymptotic -1.5 power law behavior for the threshold value $\Delta = |0.0001|$, which is typical for on-off intermittency transitions, as shown in Fig. 10.

Now we characterize the intermittency transition to GS in the present case, again by using the notion of the probability of synchronization $\Phi(b_3)$ and from the changes in the sign of *sub*Lyapunov exponents of the coupled system. The probability of synchronization is shown in Fig. 11a as a function of the coupling strength, again calculated from the response $x_2(t)$ and the auxiliary $x_3(t)$ systems, Eqs. (11b) and (11c), respectively, which remains zero in the range of $b_3 \in (0, 0.60)$ and oscillates between its maximum and minimum values in a narrow range of $b_3 \in (0.60, 0.68)$ confirming the existence of approximate CS in the later range. Above $b_3 = 0.68$ the probability of synchronization acquires its maximum value depicting perfect CS between the response $x_2(t)$ and the auxiliary $x_3(t)$ systems. Correspondingly there exists perfect GS between the drive

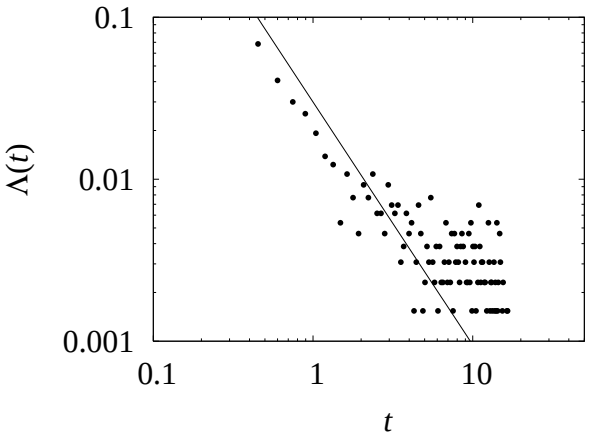

FIG. 10: The statistical distribution of laminar phases for the Fig. 9.

$x_1(t)$ and the response $x_2(t)$ systems. Fig. 11b shows the first twelve maximal Lyapunov exponents of the coupled drive $x_1(t)$ and the response $x_2(t)$ systems. The least positive *sub*Lyapunov exponent of the response system starts to become negative from $b_3 > 0.60$. Subsequently, all the other positive *sub*Lyapunov exponents become negative and reach saturation in a rather narrow range of $b_3 \in (0.60, 0.68)$. Thus the narrow range intermittency (IGS) transition (this can also be termed as immediate intermittency transition in analogy with the terminology used in [23]) is confirmed from both the probability of synchronization, calculated from the response and the auxiliary systems, and negative saturation of *sub*Lyapunov exponents, calculated from the drive and the response systems.

As discussed in the previous section, the narrow range intermittency transition is in accordance with the stabilization of all the unstable periodic orbits of the response system in a narrow range as a function of the coupling strength b_3 and this is reflected in the immediate transition of all the *sub*Lyapunov exponents (Fig. 11b) to negative values. It is also to be noted that the narrow range intermitteny transition in the case of direct feedback coupling configuration can be attributed to the fact that the strength of the coupling b_3 contributes significantly proportional to the strength of the signal $x_1(t)$ to stabilize all the UPO's immediately at the transition regime after certain threshold value of the coupling strength as in the case of low-dimensional systems [23].

The robustness of the intermittency transition in a narrow range of the coupling strength b_3 for a range of values of the parameter $b_2 \in (1.1, 1.6)$ and the delay $\tau_1 = \tau_2 \in (10, 20)$ is shown in Fig. 12. The 3-dimensional plot of the probability of synchronization as a function of the system parameter b_2 and the coupling strength b_3 is shown in Fig. 12a, while Fig. 12b shows the 3-dimensional plot of $\Phi(b_3)$ as a function of the coupling delay τ_2 and the coupling strength b_3.

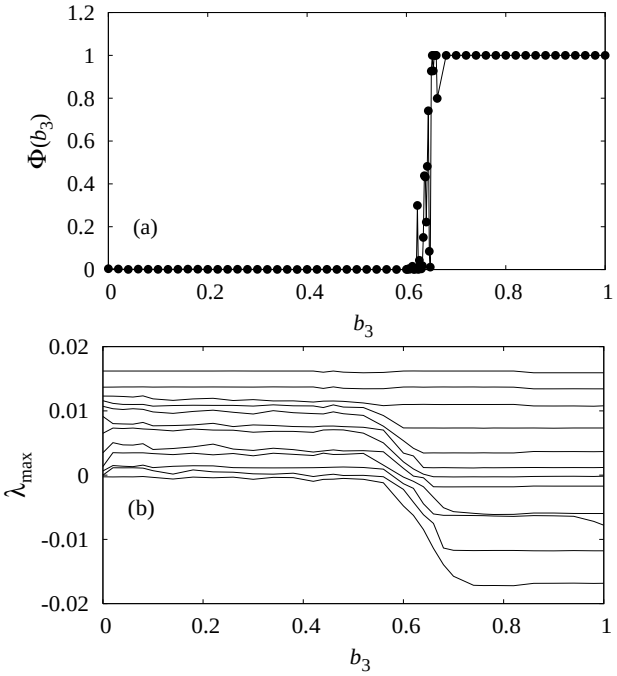

FIG. 11: (a) The probability of synchronization $\Phi(b_3)$ between the response $x_2(t)$ (11b) and the auxiliary $x_3(t)$ (11c) systems and (b) Largest Lyapunov exponents of the coupled drive $x_1(t)$ and response $x_2(t)$ systems (11a) and (11b).

IV. BROAD RANGE INTERMITTENCY TRANSITION TO GS FOR NONLINEAR ERROR FEEDBACK COUPLING OF THE FORM $(f(x_1(t-\tau_2)) - f(x_2(t-\tau_2)))$

Next we demonstrate the existence of the above types of distinct characteristic transitions for nonlinear coupling configurations as well. For this purpose, we consider the unidirectional nonlinear error feedback coupling of the form

$$\dot{x}_1(t) = -ax_1(t) + b_1 f(x_1(t-\tau_1)), \tag{13a}$$

$$\dot{x}_2(t) = -ax_2(t) + b_2 f(x_2(t-\tau_2)) + b_3(f(x_1(t-\tau_2)) - f(x_2(t-\tau_2))), \tag{13b}$$

$$\dot{x}_3(t) = -ax_3(t) + b_2 f(x_3(t-\tau_2)) + b_3(f(x_1(t-\tau_2)) - f(x_3(t-\tau_2))), \tag{13c}$$

where $f(x)$ is again of the same piece-wise linear form as in Eq. (2). The parameters are now fixed as $a = 1.0, b_1 = b_2 = 1.2, \tau_1 = 20$ and the coupling delay $\tau_2 = 25$, where the delays alone form the parameter mismatch between the drive and response systems in Eqs. (13). Following Krasvoskii-Lyapunov theory, for complete synchronization so that the manifold $\Delta = x_3(t) - x_2(t)$ between the response $x_2(t)$ and the auxiliary $x_3(t)$ approaches zero, one can obtain the stability condition as

$$a > |(b_2 - b_3) f'(x_2(t-\tau_2))|\,. \tag{14}$$

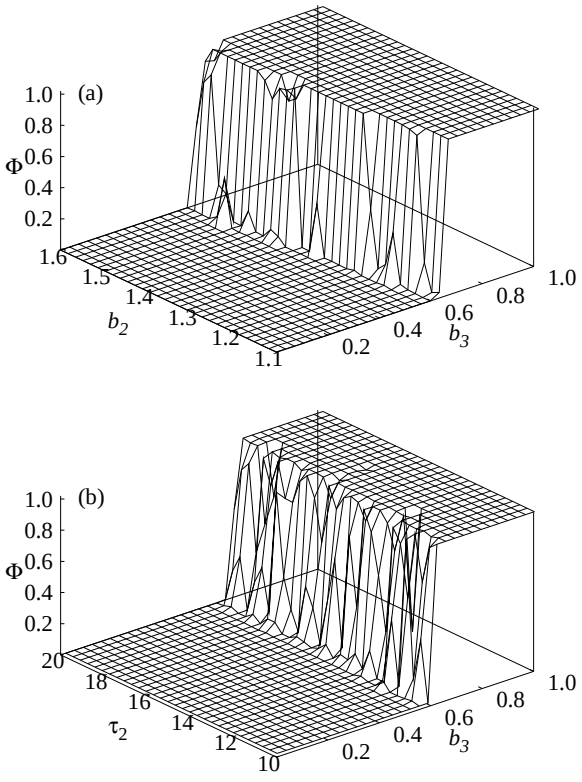

FIG. 12: The probability of synchronization $\Phi(b_3)$ in 3-dimensional plots (a) as a function of the system parameter b_2 and the coupling strength b_3 and (b) as a function of the coupling delay τ_2 and the coupling strength b_3, exhibiting narrow range intermittency transition to GS for linear direct feedback coupling

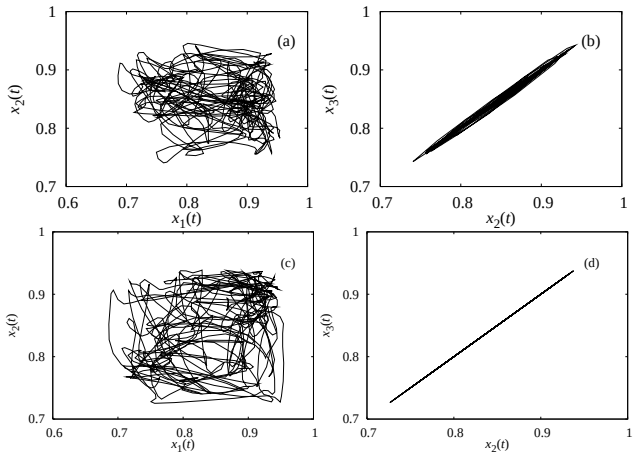

FIG. 13: Dynamics in the phase space of the systems (13)). (a) and (b): Approximate GS and CS, respectively, for the value of the coupling strength $b_3 = 0.37$. (c) and (d): Perfect GS and CS, respectively, for the value of the coupling strength $b_3 = 0.8$.

Consequently from the form of the piecewise linear function (2), the stability condition (14) becomes $a > |1.5(b_2 - b_3)| > |(b_2 - b_3)|$. Thus one can take

$$a > |b_2 - b_3| \tag{15}$$

as less stringent condition for (7) to be valid, while

$$a > |1.5b_2 - 1.5b_3| \tag{16}$$

can be considered as the most general condition specified by (14) for asymptotic stability of the synchronized state $\Delta = x_2(t) - x_3(t) = 0$. For the chosen values of the parameters, the less stringent stability condition (15) is satisfied for the values of the coupling strength $b_3 \in (0.2, 0.535)$ and the general stability condition (16) is satisfied for $b_3 > 0.535$.

As the coupling strength is increased from zero, approximate GS occurs from $b_3 > 0.2$. Figure 13a shows the approximate GS (IGS) between the drive $x_1(t)$ (Eq. (13a)) and the response $x_2(t)$ (Eq. (13b)) systems for the value of the coupling strength $b_3 = 0.37$, while the approximate CS between the response $x_2(t)$ (Eq. (13b)) and the auxiliary $x_3(t)$ (Eq. (13c)) systems is shown in Fig. (13b). Perfect GS and perfect CS are shown in Figs. 13c and 13d respectively for $b_3 = 0.8$. The intermittent dynamics exhibited by the coupled systems at the transition regime is shown in Fig. 14, which shows bursts at the period approximately equal to the delay time of the response system $x_2(t)$ for bursts of amplitude greater than $|0.01|$ (Fig. 14b). The statistical distribution of the laminar phases away from the intermittent bursts shows an asymptotic -1.5 power law behavior for the threshold value $\Delta = |0.0001|$ (see Fig. 14c), typical for on-off intermittency, which is shown in Fig. 15b. On the other hand for the threshold value $\Delta = |0.1|$ Fig. 15a shows periodic structures similar to Fig. 5a with peaks occuring approximately at $t = nT, n = 1, 2, ...$, where $T \approx \tau_2$ is the period of the lowest periodic orbit of the uncoupled system (13b).

Now, the intermittency transition is again characterized using the probability of synchronization and the *sub*Lyapunov exponents as in the previous cases. Fig. 16a shows the probability of synchronization $\Phi(b_3)$, the value of which remains zero in the range $b_3 \in (0, 0.2)$ due to the fact that there lacks any entrainment between the response $x_2(t)$ and the auxiliary $x_3(t)$ systems, whereas it fluctuates between the two extreme values in a rather broad range of the coupling strength $b_3 \in (0.2, 0.42)$, depicting the existence of intermittency transition in the corresponding range of b_3. Perfect CS exists for $b_3 > 0.42$ as evidenced from the maximum value of $\Phi(b_3)$. Correspondingly there exists perfect GS between the drive $x_1(t)$ and the response $x_2(t)$ systems. Figure 16b shows the transition of *sub*Lyapunov exponents of the spectrum of Lyapunov exponents of the coupled drive $x_1(t)$ (Eq. (13a)) and the response $x_2(t)$ (Eq. (13b)) systems. The *sub*Lyapunov exponents become negative in

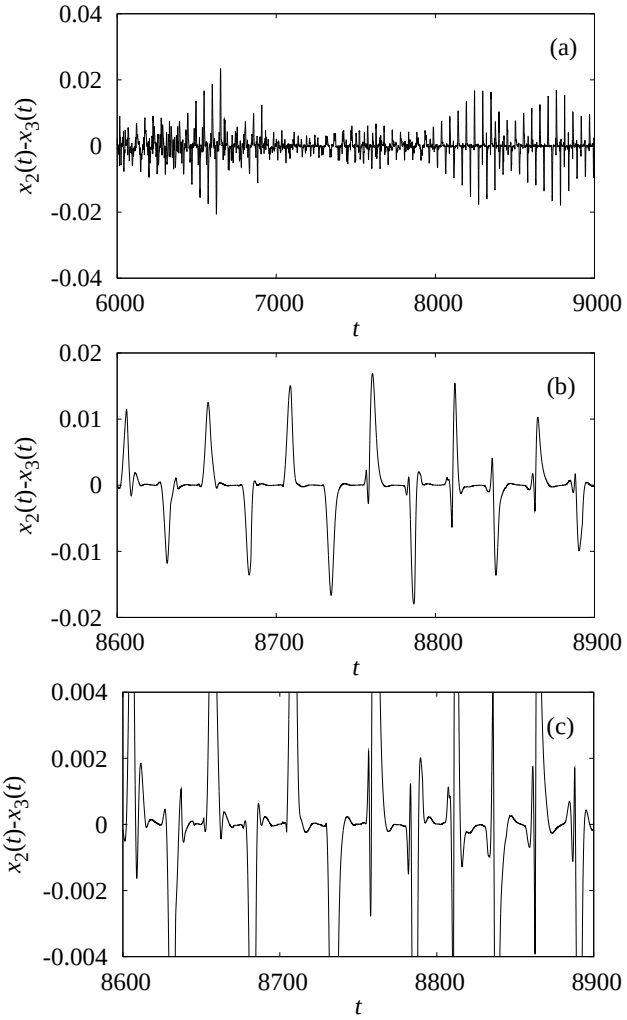

FIG. 14: The intermittent dynamics of the response $x_2(t)$ (13b) and auxiliary $x_3(t)$ (13c) systems for the the value of the coupling strength $b_3 = 0.37$ for nonlinear error feedback coupling. (a) Time traces of the difference $x_2(t) - x_3(t)$ corresponding to Fig. 13b, (b) Enlarged in x scale to show bursts at periodic intervals when bursts of larger amplitudes $\Delta > |0.01|$ are considered and (c) Enlarged in y scale to show random bursts when bursts of smaller amplitudes $\Delta < |0.01|$ are considered.

the range $b_3 \in (0.2, 0.42)$ confirming the broad range intermittency (IGS) transition in a rather wide range of the coupling strength and this is again due to the gradual stabilization of the unstable periodic orbits of the response systems because of the less significant contribution of the coupling strength b_3 as the error becomes gradually smaller from the transition regime beyond certain threshold value of the coupling strength as discussed in Sec. II. The robustness of the intermittency transition with the system parameter b_2 and the coupling delay τ_2 as a function of coupling strength b_3 is shown as 3-dimensional plots in Figs. 17.

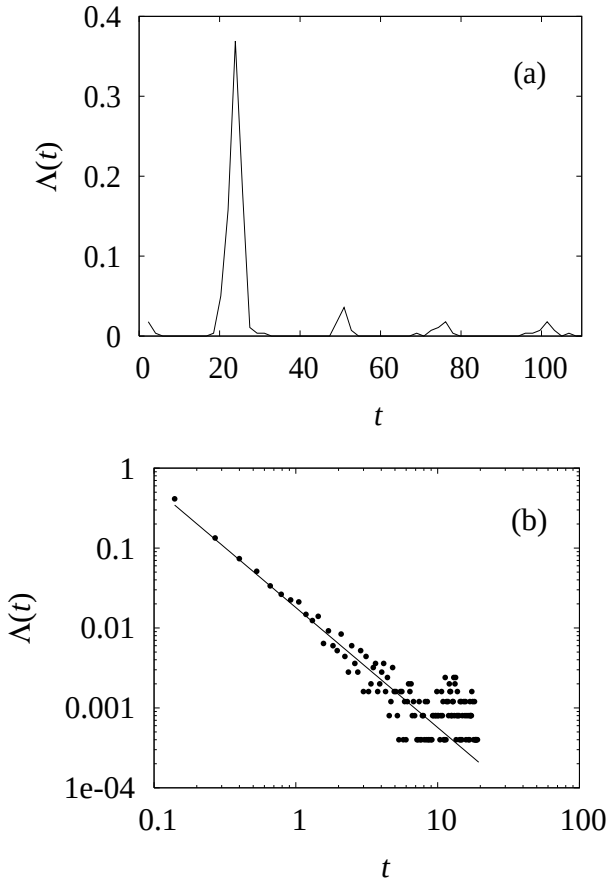

FIG. 15: The statistical distribution of laminar phases corresponding to the Fig. 14. (a) For threshold value $\Delta = |0.1|$ and (b) for the threshold value of $\Delta = |0.0001|$.

V. NARROW RANGE INTERMITTENCY TRANSITION TO GS FOR NONLINEAR DIRECT FEEDBACK COUPLING OF THE FORM $f(x_1(t-\tau_2))$

Now we consider the unidirectional nonlinear coupling of the form

$$\dot{x}_1(t) = -ax_1(t) + b_1 f(x_1(t-\tau_1)), \tag{17a}$$
$$\dot{x}_2(t) = -ax_2(t) + b_2 f(x_2(t-\tau_2)) + b_3 f(x_1(t-\tau_2)), \tag{17b}$$
$$\dot{x}_3(t) = -ax_3(t) + b_2 f(x_3(t-\tau_2)) + b_3 f(x_1(t-\tau_2)). \tag{17c}$$

Choosing the values of the parameters as in the previous case and following Krasvoskii-Lyapunov functional approach for the asymptotically stable synchronized state $\Delta = x_3(t) - x_2(t) = 0$, one can obtain the sufficient condition for asymptotic stability for complete synchronization of the response $x_2(t)$ and the auxiliary $x_3(t)$ systems as

$$a > |b_2 f'(x_2(t-\tau_2))|\,. \tag{18}$$

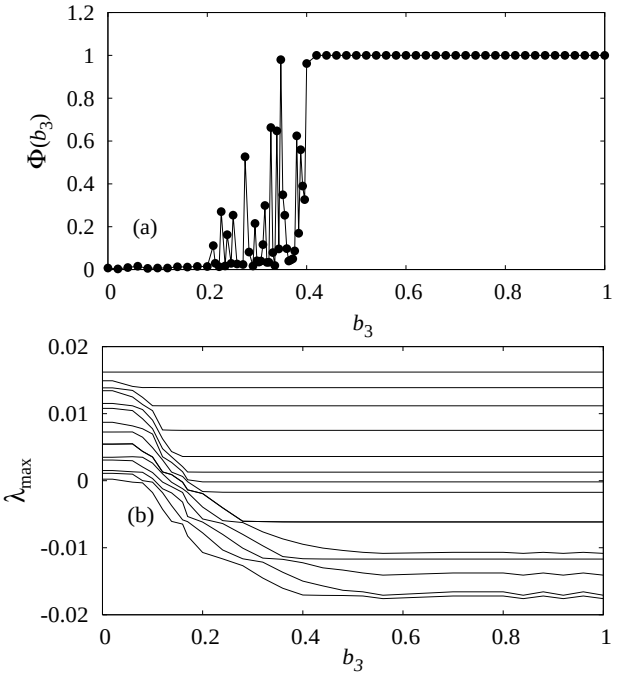

FIG. 16: (a) The probability of synchronization $\Phi(b_3)$ between the response $x_2(t)$ (13b) and the auxiliary $x_3(t)$ (13c) systems and (b) Largest Lyapunov exponents of the coupled drive $x_1(t)$ and response $x_2(t)$ systems (13a) and (13b).

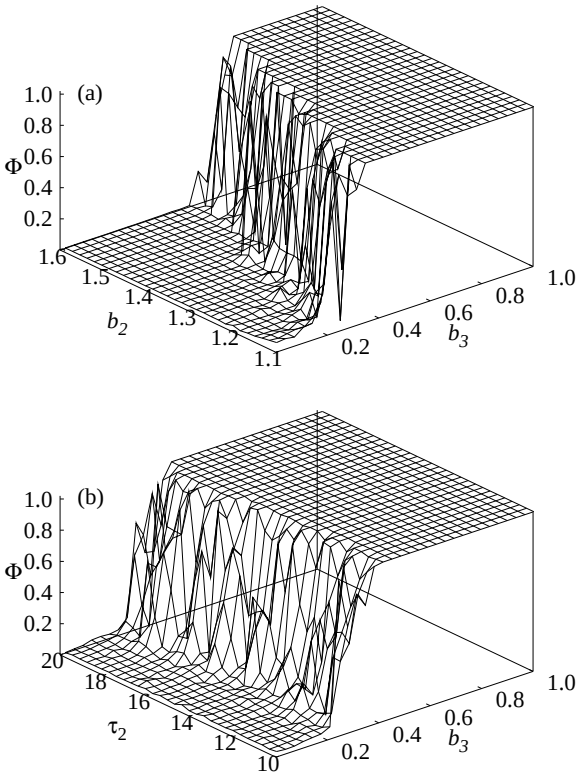

FIG. 17: The probability of synchronization $\Phi(b_3)$ in 3-dimensional plots (a) as a function of the system parameter b_2 and the coupling strength b_3 and (b) as a function of the coupling delay τ_2 and the coupling strength b_3 for the case of nonlinear error feedback coupling configuration given by Eq. (13), showing broad range intermittency transition.

The above stability condition rapidy leads to immediate transition to synchronized state even for very feeble values of the coupling strength b_3 for the parameter values satisfying the stability condition (18) as the stability condition is independent of b_3 as in the previous linear coupling case (Sec. III). Hence it is difficult to identify the possible dynamical transitions to synchronized state as a function of the coupling strength b_3. Hence we study the synchronization transition as a function of the coupling strength b_3 by choosing the parameters violating the stability condition as $a = 1.0, b_1 = 1.2, b_2 = 1.1$ and $\tau_1 = \tau_2 = 15$.

As b_3 is varied from zero for the above values of the parameters, transition from desynchronized state to approximate GS occurs for $b_3 > 0.74$. The approximate GS (IGS) between the drive $x_1(t)$ and the response $x_2(t)$ variables described by Eqs.(17a) and (17b) is shown in Fig. 18a, whereas Fig. 18b shows the approximate CS between the response $x_2(t)$ and the auxiliary $x_3(t)$ variables (Eqs. (17a) and (17c)) for the value of the coupling strength $b_3 = 0.78$. Perfect GS and perfect CS are shown in Figs. 18c and 18d respectively for $b_3 = 0.9$. Time traces of the difference $x_2(t) - x_3(t)$ corresponding to approximate CS (Fig. 18b) is shown in Fig. 19, which shows intermittent dynamics with the entrainment of the dynamical variables in random time intervals of finite duration. Fig. 19b shows the enlarged picture of part of Fig. 19a. The statistical distribution of the laminar phases again shows a universal asymptotic -1.5 power

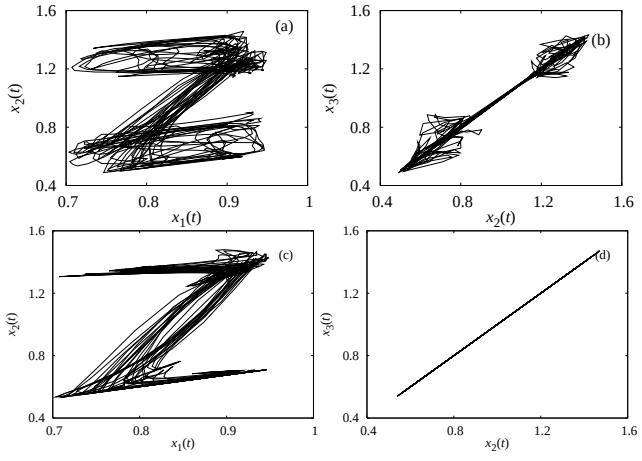

FIG. 18: Dynamics in the phase space of the systems (17)). (a) and (b): Approximate GS and CS, respectively, for the value of the coupling strength $b_3 = 0.78$. (c) and (d): Perfect GS and CS, respectively, for the value of the coupling strength $b_3 = 0.9$.

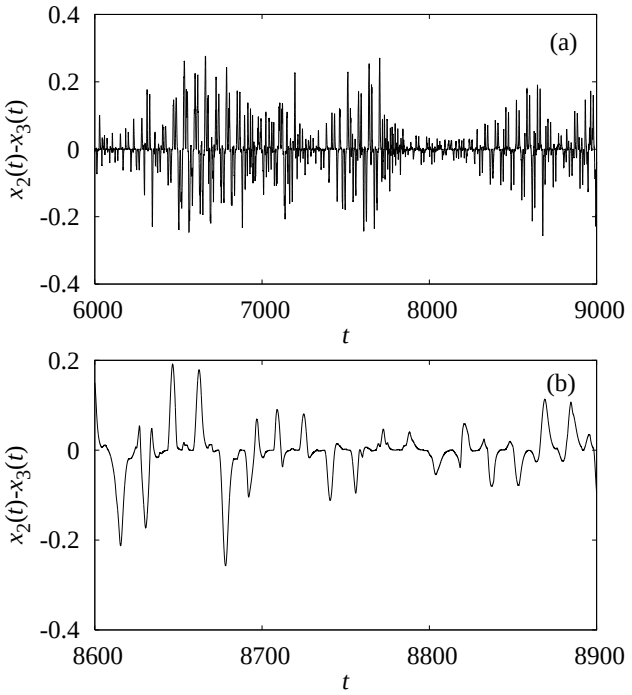

FIG. 19: The intermittent dynamics of the response $x_2(t)$ (17b) and auxiliary $x_3(t)$ (17c) systems for the the value of the coupling strength $b_3 = 0.78$. (a) and (b) Time traces of the difference $x_2(t) - x_3(t)$ corresponding to Fig. 18b.

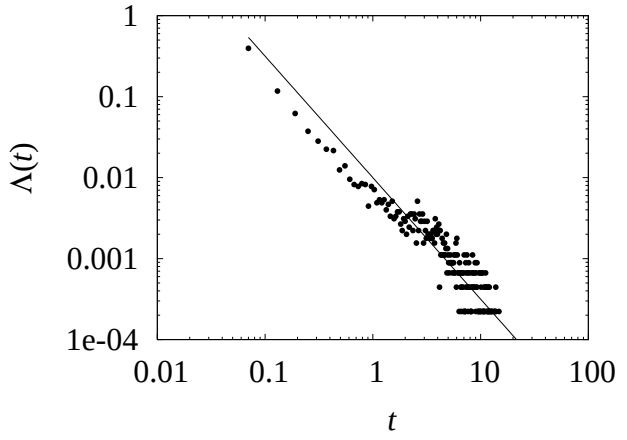

FIG. 20: The statistical distribution of laminar phase for the Fig. 19.

law behavior for the threshold value $\Delta = |0.0001|$, typical for on-off intermittency, as shown in Fig. 20.

As in the previous cases, now we characterize the intermittency transition to GS using the notion of probability of synchronization $\Phi(b_3)$ and from the changes in the sign of *sub*Lyapunov exponents in the spectrum of Lyapunov exponents of the coupled time-delay systems (17). Fig. 21a shows the probability of synchronization $\Phi(b_3)$ as a function of the coupling strength

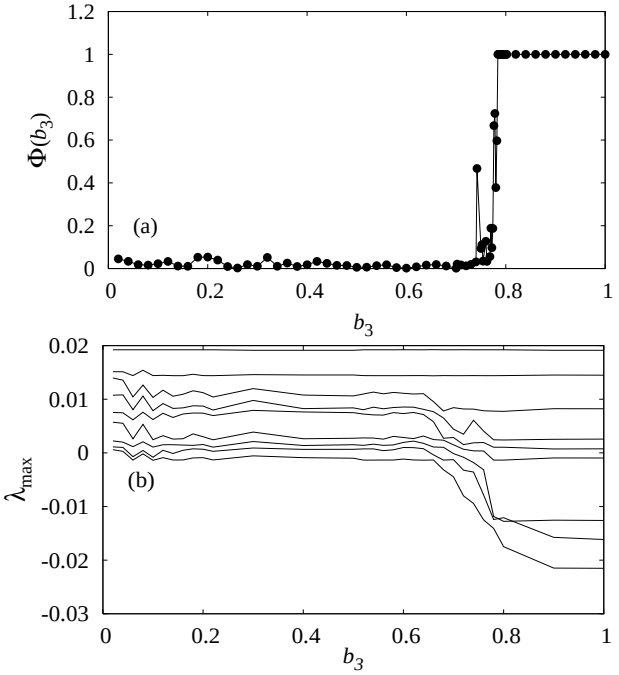

FIG. 21: (a) The probability of synchronization $\Phi(b_3)$ between the response $x_2(t)$ (17b) and the auxiliary $x_3(t)$ (17c) systems and (b) Largest Lyapunov exponents of the coupled drive $x_1(t)$ and response $x_2(t)$ systems (17a) and (17b).

b_3 calculated from the response $x_2(t)$ and the auxiliary $x_3(t)$ variables (Eqs. (17b) and (17c)) for CS between them. In the range of $b_3 \in (0, 0.74)$, the probability of synchronization remains approximately zero. Upon increasing the value of b_3, $\Phi(b_3)$ oscillates in the narrow range of $b_3 \in (0.74, 0.78)$ depicting the existence of intermittency transition. This narrow range transition is also confirmed from the transition of successive largest *sub*Lyapunov exponents. The spectrum of the first nine largest Lyapunov exponents λ_{max} of the coupled drive $x_1(t)$ and response $x_2(t)$ variables (Eqs. (17a) and (17b)) is shown in Fig. 21b. It is also evident from the spectrum that the *sub*Lyapunov exponents suddenly become negative in the narrow range of $b_3 \in (0.74, 0.78)$, and then reach saturation values for $b_3 > 0.78$. This confirms the narrow range intermittency (IGS) transition to GS. This is also in accordance with the immediate stabilization of all the UPO's of the response system as discussed in Sec. (III).

The robustness of the transition with the system parameter b_2 and the delay time τ_2 as a function of coupling strength b_3 is shown as 3-dimensional plots in Fig. 22.

VI. CONCLUSION

In conclusion, we have studied intermittency transition to generalized synchronization from desynchronized state in unidirectionally coupled scalar piecewise linear time-

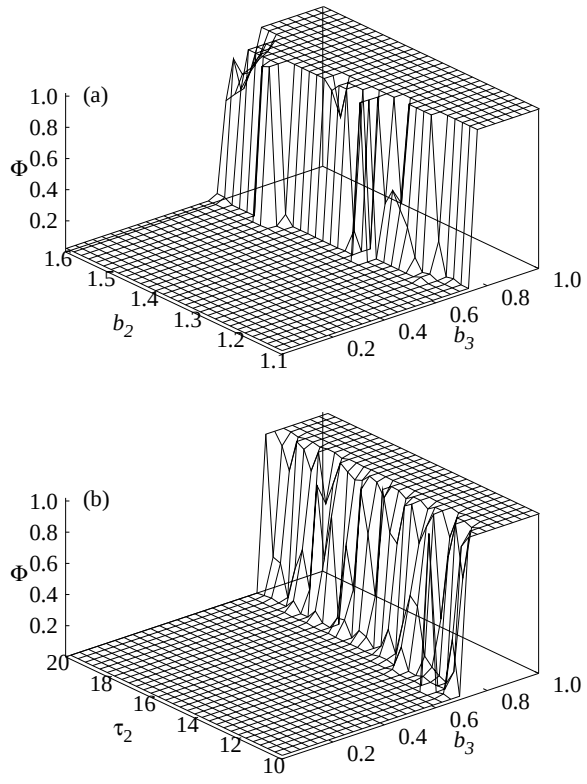

FIG. 22: The probability of synchronization $\Phi(b_3)$ in 3-dimensional plots (a) as a function of the system parameter b_2 and the coupling strength b_3 and (b) as a function of the coupling delay τ_2 and the coupling strength b_3 for the case of nonlinear direct feedback coupling configuration given by Eq. (17) showing narrow range intermittency transition to GS.

delay systems for different coupling configurations using the auxiliary system approach. We have shown that the intermittency transition to GS occurs in a broad range of coupling strength for both linear and nonlinear error feedback coupling configurations whereas it occurs in a narrow range of coupling strength for both the linear and nonlinear direct feedback coupling configuration. It has also been shown that the intermittent dynamics displays periodic intermittent bursts of period equal to the delay time of the response systems in the former cases and it takes place in random time intervals in the latter cases. The robustness of the intermittent dynamics with the system parameters and the delay time is also studied as a function of the coupling strength for both error feedback and direct feedback (linear and nonlinear) coupling configurations. Universality of these intermittent behaviors [36] (periodic and random) and their (broad and narrow range) transitions are also confirmed for different forms of linear and nonlinear coupling configurations in other time-delay systems such as Mackey-Glass and Ikeda systems. These distinct characteristic behaviors are analyzed using the analytical stability condition for synchronized state, probability of synchronization $\Phi(b_3)$ between the response and the auxiliary systems, and by the changes in the sign of *sub*Lyapunov exponents in the spectrum of Lyapunov exponents of the drive and the response systems in both the linear and nonlinearly coupled time-delay systems. In spite of the fact that both the probability of synchronization and the *sub*Lyapunov exponents have been calculated from different systems, we have found good agreement between them in showing intermittency transition in all the cases. We hope this study will contribute to the basic understanding of the nature of transition to GS in coupled time-delay systems and we are now investigating the experimental verification of these findings in nonlinear electronic circuits.

Acknowledgments

The work of D. V. S and M. L has been supported by a Department of Science and Technology, Government of India sponsored research project. The work of M. L is supported by a DAE-BRNS Raja Ramanna Fellowship award, India.

APPENDIX A: STABILITY CONDITION

To estimate a sufficient condition for the stability of the solution $\Delta = 0$, we require the derivative of the functional $V(t)$ along the trajectory of Eq. (4),

$$\frac{dV}{dt} = -(a+b_3)\Delta^2 + b_2 f'(x_2(t-\tau_2))\Delta\Delta_{\tau_2} + \mu\Delta^2 - \mu\Delta_{\tau_2}^2, \tag{A1}$$

to be negative. The above equation can be rewritten as

$$\frac{dV}{dt} = -\mu\Delta^2\Gamma(X,\mu), \tag{A2}$$

where $X = \Delta_{\tau_2}/\Delta$, $\Gamma = \big[\big((a+b_3-\mu)/\mu\big) - \big(b_2 f'(x_2(t-\tau_2))/\mu\big)X + X^2\big]$. In order to show that $\frac{dV}{dt} < 0$ for all Δ and Δ_{τ_2} and so for all X, it is sufficient to show that $\Gamma_{min} > 0$. One can easily check that the absolute minimum of Γ occurs at $X = \frac{1}{2\mu} b_2 f'(x_2(t-\tau_2))$ with $\Gamma_{min} = \big[4\mu(a+b_3-\mu) - b_2^2 f'(x_2(t-\tau_2))^2\big]/4\mu^2$. Consequently, we have the condition for stability as

$$a + b_3 > \frac{b_2^2 f'(x_2(t-\tau_2))^2}{4\mu} + \mu = \Phi(\mu). \tag{A3}$$

Again $\Phi(\mu)$ as a function of μ for a given $f'(x)$ has an absolute minimum at $\mu = (|b_2 f'(x_2(t-\tau_2))|)/2$ with $\Phi_{min} = |b_2 f'(x_2(t-\tau_2))|$. Since $\Phi \geq \Phi_{min} = |b_2 f'(x_2(t-\tau_2))|$, from the inequality (A3), it turns out that the sufficient condition for asymptotic stability is

$$a + b_3 > |b_2 f'(x_2(t-\tau_2))|. \tag{A4}$$

Now from the form of the piecewise linear function $f(x)$ given by Eq. 2, we have,

$$|f'(x_2(t-\tau_2))| = \begin{cases} 1.5, & 0.8 \leq |x_2| \leq \frac{4}{3} \\ 1.0, & |x_2| < 0.8 \end{cases} \quad \text{(A5)}$$

Note that the region $|x_2| > 4/3$ is outside the dynamics of the present system (see Eq. (2)). Consequently the stability condition (A4) becomes $a + b_3 > 1.5|b_2| > |b_2|$.

Thus one can take $a + b_3 > |b_2|$ as a less stringent condition for (A4) to be valid, while

$$a > 1.5|b_2|, \quad \text{(A6)}$$

as the most general condition specified by (A4) for asymptotic stability of the synchronized state $\Delta = 0$.

[1] A. S. Pikovsky, M. G. Rosenblum, and J. Kurths, *Synchronization - A Unified Approach to Nonlinear Science* (Cambridge University Press, Cambridge, 2001).
[2] S. Boccaletti, J. Kurths, G. Osipov, D. L. Valladares, and C. S. Zhou, Phys. Rep. **366**, 1 (2002).
[3] H. Fujisaka and T. Yamada, Prog. Theor. Phys. **69**, 32 (1983).
[4] H. Fujisaka and T. Yamada, Prog. Theor. Phys. **70**, 1240 (1983).
[5] L. M. Pecora and T. L. Carroll, Phys. Rev. Lett. **64**, 821 (1990).
[6] R. Brown and L. Kocarev, Chaos **10**, 344 (2000).
[7] S. Boccaletti, L. M. Pecora, and A. Pelaez, Phys. Rev. E **63**, 066219 (2001).
[8] A. E. Hramov and A. A. Koronovskii, Chaos **14**, 603 (2004).
[9] N. F. Rulkov, M. M. Sushchik, L. S. Tsimring, and H. D. I.Abarbanel, Phys. Rev. E **51**, 980 (1995).
[10] H. D. I. Abarbanel, N. F. Rulkov, and M. M. Sushchik, Phys. Rev. E **53**, 4528 (1996).
[11] R. Brown, Phys. Rev. Lett. **81**, 4835 (1998).
[12] L. Kocarev and U. Parlitz, Phys. Rev. Lett. **76**, 1816 (1996).
[13] K. Pyragas, Phys. Rev. E **54**, R4508 (1996).
[14] B. R. Hunt, E. Ott, and J. A. Yorke, Phys. Rev. E **55**, 4029 (1997).
[15] N. F. Rulkov and C. T. Lewis, Phys. Rev. E **63**, 065204(R) (2001).
[16] A. E. Hramov, A. A. Koronovskii, and P. V. Popov, Phys. Rev. E **72**, 037201 (2005).
[17] A. E. Hramov and A. A. Koronovskii, Euro Physics Letter **79**, 169 (2005).
[18] S. Boccaletti and D. L. Valladares, Phys. Rev. E **62**, 7497 (2000).
[19] D. L. Valladares, S. Boccaletti, and M. F. Carusela, Int. J. Bifurcation and Chaos **11**, 2699 (2001).
[20] A. Pikovsky, G. Osipov, M. Rosenblum, M. Zaks, and J. Kurths, Phys. Rev. Lett. **79**, 47 (1997).
[21] A. Pikovsky, M. Zaks, M. Rosenblum, G. Osipov, and J. Kurths, Chaos **7**, 680 (1997).
[22] K. J. Lee, Y. Kwak, and T. K. Lim, Phys. Rev. Lett. **81**, 321 (1998).
[23] L. Zhao, Y. C. Lai, and C. W. Shih, Phys. Rev. E **72**, 036212 (2005).
[24] M. Zhan, X. Wang, X. Gong, G. W. Wei, and C. H. Lai, Phys. Rev. E **68**, 036208 (2003).
[25] E. M. Shahverdiev and K. A. Shore, Phys. Rev. E **71**, 016201 (2005).
[26] D. V. Senthilkumar, M. Lakshmanan, and J. Kurths, Phys. Rev. E **74**, 035205(R) (2006).
[27] D. V. Senthilkumar and M. Lakshmanan, Phys. Rev. E **71**, 016211 (2005).
[28] H. Lu and Z. He, IEEE Trans. Circuits Syst. I **43**, 700 (1996).
[29] P. Thangavel, K. Murali, and M. Lakshmanan, Int. J. Bifurcation and Chaos **8**, 2481 (1998).
[30] D. V. Senthilkumar and M. Lakshmanan, Int. J. Bifurcation and Chaos **15**, 2895 (2005).
[31] J. D. Farmer, Physica D **4**, 366 (1982).
[32] N. N. Krasovskii, *Stability of Motion* (Stanford University Press, Stanford, 1963).
[33] K. Pyragas, Phys. Rev. E **58**, 3067 (1998).
[34] N. Platt, S. M. Hammel, and J. F. Heagy, Phys. Rev. Lett **72**, 3498 (1994).
[35] J. F. Heagy, N. Platt, and S. M. Hammel, Phys. Rev. E **49**, 1140 (1994).
[36] M. Lakshmanan and R. Sahadevan(Eds.), *Proceedings of the Third National Conference on Nonlinear Systems and Dynamics,* (Allied Publishers, Chennai, 2006).